



**HAL**  
open science

## Seizure activity triggers tau hyperphosphorylation and amyloidogenic pathways

Geoffrey Canet, Emma Zub, Charleine Zussy, Célia Hernandez, Marine Blaquière, Valentin Garcia, Mathieu Vitalis, Frédéric de Bock, Maria Moreno-montano, Etienne Audinat, et al.

### ► To cite this version:

Geoffrey Canet, Emma Zub, Charleine Zussy, Célia Hernandez, Marine Blaquière, et al.. Seizure activity triggers tau hyperphosphorylation and amyloidogenic pathways. *Epilepsia*, 2022, 63 (4), pp.919-935. 10.1111/epi.17186 . hal-03594983

**HAL Id: hal-03594983**

**<https://hal.science/hal-03594983>**




Submitted on 7 Oct 2022

**HAL** is a multi-disciplinary open access archive for the deposit and dissemination of scientific research documents, whether they are published or not. The documents may come from teaching and research institutions in France or abroad, or from public or private research centers.

L'archive ouverte pluridisciplinaire **HAL**, est destinée au dépôt et à la diffusion de documents scientifiques de niveau recherche, publiés ou non, émanant des établissements d'enseignement et de recherche français ou étrangers, des laboratoires publics ou privés.

## RESEARCH ARTICLE

# Seizure activity triggers tau hyperphosphorylation and amyloidogenic pathways

Geoffrey Canet<sup>1,2</sup>  | Emma Zub<sup>2</sup> | Charleine Zussy<sup>1</sup> | Célia Hernandez<sup>1</sup> |  
 Marine Blaquiére<sup>3</sup> | Valentin Garcia<sup>3</sup> | Mathieu Vitalis<sup>1</sup> | Frederic deBock<sup>3</sup> |  
 Maria Moreno-Montano<sup>3</sup> | Etienne Audinat<sup>3</sup> | Catherine Desrumaux<sup>1</sup> |  
 Emmanuel Planel<sup>2</sup> | Laurent Givalois<sup>1,2</sup>  | Nicola Marchi<sup>3</sup> 

<sup>1</sup>Molecular Mechanisms in Neurodegenerative Dementia Laboratory, University of Montpellier, EPHE-PSL, INSERM U1198, Montpellier, France

<sup>2</sup>Department of Psychiatry and Neurosciences, Laval University, CR-CHU of Québec, Québec, Canada

<sup>3</sup>Institute of Functional Genomics, University of Montpellier, UMR 5203 CNRS – U 1191 INSERM, Montpellier, France

## Correspondence

Dr Nicola Marchi, Cerebrovascular and Glia Research, Institut de Génétique Fonctionnelle (CNRS UMR5203, INSERM U1191, University of Montpellier), 141 rue de la Cardonille, 34094 Montpellier, Cedex 5, France.  
 Email: [nicola.marchi@igf.cnrs.fr](mailto:nicola.marchi@igf.cnrs.fr)

Dr Laurent Givalois, Molecular Mechanisms in Neurodegenerative Dementia (MMDN) Laboratory, University of Montpellier, U1198 INSERM, Team Environmental Impact in Alzheimer's Disease (EiAlz), Place E. Bataillon, 34095 Montpellier, France.  
 Email: [laurent.givalois@umontpellier.fr](mailto:laurent.givalois@umontpellier.fr)

## Funding information

Agence Nationale de la Recherche

## Abstract

**Objective:** Although epilepsies and neurodegenerative disorders show pathophysiological similarities, their direct functional associations are unclear. Here, we tested the hypothesis that experimental seizures can induce tau hyperphosphorylation and amyloidogenic modifications over time, with intersections with neuroinflammation.

**Methods:** We used a model of mesial temporal lobe epilepsy (MTLE) where unilateral intrahippocampal injection of kainic acid (KA) in C57BL/6 mice elicits epileptogenesis and spontaneous focal seizures. We used a model of generalized status epilepticus (SE) obtained by intraperitoneal KA injection in C57BL/6 mice. We performed analyses and cross-comparisons according to a schedule of 72 h, 1 week, and 8 weeks after KA injection.

**Results:** In experimental MTLE, we show AT100, PHF1, and CP13 tau hyperphosphorylation during epileptogenesis (72 h–1 week) and long-term (8 weeks) during spontaneous seizures in the ipsilateral hippocampi, the epileptogenic zone. These pathological modifications extended to the contralateral hippocampus, a seizure propagating zone with no histological lesion or sclerosis. Two kinases, Cdk5 and GSK3 $\beta$ , implicated in the pathological phosphorylation of tau, were activated. In this MTLE model, the induction of the amyloidogenic pathway (APP, C99, BACE1) was prominent and long-lasting in the epileptogenic zone. These Alzheimer's disease (AD)-relevant markers, established during seizure progression and recurrence, reciprocated an enduring glial (GFAP, Iba1) inflammation and the inadequate activation of the endogenous, anti-inflammatory, glucocorticoid receptor system. By contrast, a generalized SE episode provoked a predominantly transient induction of tau hyperphosphorylation and amyloidogenic markers in the hippocampus, along with resolving inflammation. Finally, we identified overlapping profiles of long-term hippocampal tau hyperphosphorylation by comparing MTLE to J20 mice, the latter a model relevant to AD.

[Corrections added on 19 July, 2022, after first online publication: The copyright line has been changed.]

This is an open access article under the terms of the [Creative Commons Attribution-NonCommercial](https://creativecommons.org/licenses/by-nc/4.0/) License, which permits use, distribution and reproduction in any medium, provided the original work is properly cited and is not used for commercial purposes.

© 2022 The Authors. *Epilepsia* published by Wiley Periodicals LLC on behalf of International League Against Epilepsy.

**Significance:** MTLE and a generalized SE prompt persistent and varying tau hyperphosphorylation or amyloidogenic modifications in the hippocampus. In MTLE, an AD-relevant molecular trajectory intertwines with neuroinflammation, spatiotemporally involving epileptogenic and nonlesional seizure propagating zones.

**KEYWORDS**

amyloid, epileptogenesis, neurodegeneration, neuroinflammation, status epilepticus, tau phosphorylation, temporal lobe epilepsy

## 1 | INTRODUCTION

A bidirectional link between seizure and neurodegenerative disorders has clinically emerged<sup>1–4</sup> and is debated.<sup>5</sup> Poorly controlled seizures represent a risk factor for neurodegeneration, supporting the concept of an epileptic prodrome.<sup>4,6</sup> In Alzheimer's disease (AD), an increased risk of seizures at early or even presymptomatic stages exists.<sup>7</sup> AD is a principal neurodegenerative pathology presenting amyloid- $\beta$  peptide extracellular aggregates and neurofibrillary tangles of hyperphosphorylated tau. Notably, amyloidogenic and tau-related markers are reported in brain specimens obtained from subjects with temporal lobe epilepsy (TLE), along with a diagnosis of cognitive comorbidities reminiscent of neurodegenerative settings.<sup>1,2,4</sup> The exact prevalence of amyloid plaques and phospho-tau in the human TLE brain remains debated.<sup>5</sup> In general, clinical studies support the notion of overlapping pathological elements between specific epilepsies and neurodegenerative disorders.<sup>4</sup>

Here, we tested the hypothesis that experimental seizure progression, induced in an otherwise normal brain, elicits amyloidogenic and tau-related pathological markers and trajectories. We used a model of mesial TLE (MTLE) based on unilateral intrahippocampal (ih) kainic acid (KA) injection in C57BL/6 mice. This model leads to epileptogenesis and the development of spontaneous focal seizures.<sup>8–11</sup> The KA-injected ipsilateral hippocampus is the epileptogenic zone presenting significant sclerosis.<sup>9,12</sup> The contralateral, noninjected, hippocampus is a seizure propagation zone devoid of lesion or sclerosis.<sup>8</sup> In parallel, we tested whether a generalized status epilepticus (SE) episode is sufficient to trigger proamyloidogenic and tau-related modifications over time. To this end, we included a model of generalized SE based on intraperitoneal (ip) injection of KA in C57BL/6 mice.<sup>13</sup> With this approach, SE occurs as one event that does not lead to epileptogenesis in this specific mouse strain.<sup>13</sup> By cross-comparing MTLE and SE models and outcomes, we identified the contributions of epileptogenesis, hippocampal sclerosis, and seizure propagation in modifying the expression of selected AD-relevant

### Key points

- In MTLE, tau hyperphosphorylation occurs at the epileptogenic and nonlesional seizure propagating hippocampi
- A generalized SE elicited time-dependent amyloidogenic and tau hyperphosphorylation trajectories
- In MTLE, inflammation offsets an endogenous anti-inflammatory mechanism, perhaps contributing to tau hyperphosphorylation
- MTLE and AD-relevant models present overlapping neurodegenerative markers

markers. Within this specific framework,<sup>8</sup> we performed a battery of molecular and neurophysiological examinations to outline tau phosphorylation and amyloidogenic modifications, intersecting with pro- and anti-inflammatory equilibriums as a function of time and regionally.

## 2 | MATERIALS AND METHODS

### 2.1 | Animals and experimental models

C57BL/6J male mice (8–10 weeks, Janvier Laboratory) were housed in individual cages after surgery with food and water ad libitum and maintained at a 12-h light–dark cycle (room temperature =  $22 \pm 1^\circ\text{C}$ ). Animal procedures were performed according to European Committee Council Directive 2010/63/EU and after validation by our local ethical committee and the French Ministry of Research. All experiments, including euthanasia, were performed between 9 a.m. and 2 p.m. during the daily portion of the circadian rhythm. We used male mice because, in females, the estrous cycle could impact the establishment of the epileptic models.

To induce MTLE, a stereotaxic injection of 50 nl of a  $20 \text{ mmol}\cdot\text{L}^{-1}$  solution of KA (1 nmol, Sigma-Aldrich) was

performed into the right dorsal hippocampus under general anesthesia (ketamine/xylazine in sterile .9% NaCl) as previously described,<sup>8-10,14</sup> whereas sham mice received .9% NaCl. After KA injection, asymmetric clonic movements of the forelimbs and head deviations, rotations, and periods of immobility occur for several hours. These archetypical behavioral modifications lead to electrographic spontaneous seizures in 90% of the animals, as we and others previously showed by ih recordings.<sup>8,14</sup> Animals that did not exhibit these signs were excluded from the study. For ih recordings, bipolar electrodes were used, made of two insulated tungsten wires twisted together. For cortical recordings, two microscrews (.10 inches, Pinnacle Medical Equipment) were anchored to the skull (frontoparietal). A silver wire was positioned in the cerebellum as a reference electrode. Wires were connected to a prefabricated connector (Pinnacle Medical Equipment 6-pin connector), fixed, and isolated using dental acrylic cement (Palladur). Seizure or spike activity regional propagation was confirmed by placing bipolar electrodes in the contralateral hippocampi (anteroposterior = -2, lateral = -1.5 or +1.5, depth = -2 mm). Mice were monitored by video-electroencephalography (EEG) during epileptogenesis and spontaneous seizures (12 h/week, one session starting in the morning; Figure 1A).<sup>8</sup> Figure S4 provides examples of spontaneous seizure frequency, consistent with previous reports.<sup>10,11,13,14</sup>

To induce a generalized SE, ip KA injections of a maximum of 25 mg/Kg were performed (15, 5, and 5 mg/kg) within 60–90 min. This protocol leads to behavioral (head nodding to forepaw/legs clonus, arching, and falling) and electrographic generalized SE (Figure 2A) in 70%–80% of animals during a time frame of 90 min. In this model, we performed longitudinal ih and cortical EEG monitoring, confirming no epileptogenesis and spontaneous chronic seizures in C57BL/6 mice, as previously reported.<sup>13</sup> Post-SE (Figure 2A), we found hippocampal spike activity, the latter becoming sporadic long-term (8 weeks) in most animals (Figure S4), agreeing with current literature.<sup>12,13</sup> Over time, the EEG pattern after generalized SE sharply contrasts with the MTLE model, the latter leading to epileptogenesis and recurrent focal seizures (Figure 1A).<sup>8,11,14</sup>

Adult male J20 mice (hAPP<sub>Sw/Ind</sub><sup>15</sup>; Material Transfert Agreement #UM140255-01, Gladstone Institute) were bred in our animal facility (CECEMA, University of Montpellier) under standard conditions and were backcrossed for >10 generations. J20 male mice were mated with C57BL/6J female mice (Janvier Laboratory) to obtain sufficient animals for the study. Wild-type (WT) animals issued from the same litters were included as controls. Nine-month-old male mice (WT and J20) were used. For brain tissue harvesting (quantitative polymerase chain reaction [qPCR]), deeply anesthetized (ketamine/xylazine) mice

were perfused by intracardiac cold saline. For Western blot analysis of phosphorylated brain proteins and blood collection, samples were processed as previously described.<sup>16,17</sup> When needed (e.g., failure of EEG implant, suffering), euthanasia was performed using CO<sub>2</sub> inhalation.

## 2.2 | Behavioral tests

**Nesting:** In mice, nest-building is a specific form of active interaction with the environment, for shelter and temperature control. Mice were individually housed on sawdust in standard cages. One piece of cotton (5 × 5 cm) was introduced into each animal cage 3 h before the dark phase. The following day, nest-building behavior was scored according to a described rating scale of 1–5 (Figure 4A).<sup>18</sup> This test characterizes the overall animal welfare.

**Spontaneous alternation in a Y-maze:** Testing was executed in a Y-shaped maze with three white opaque plastic arms at a 120° angle (Figure 4B).<sup>18</sup> After being introduced to the maze's center, the animal freely explored the three arms for 8 min. The number of arm entries and the number of triads were recorded to calculate the percentage of alternation (Noldus EthoVisionXT video-tracking system). The apparatus was cleaned with diluted ethanol (50%) between sessions.

Spatial learning and memory were assessed using the Barnes maze,<sup>19</sup> a circular table (1 m) with 20 circular holes (5 cm) around the circumference (Figure 4C). The goal for each mouse is, with the aid of visual cues, to reach an escape box positioned beneath one of the holes. The table's surface is brightly lit, serving as an aversive stimulus that motivates the mouse to find, and hide in, the escape box. After habituation (3 min), training took place in three trials (3 min) per day for 4 days. Next, a probe test was performed (escape box was removed), and each mouse was allowed to explore for 3 min. Each trial was recorded using the Noldus EthoVisionXT video-tracking system, and several parameters were measured: escape latency, distance moved, and latency to the escape hole (probe test). The apparatus was cleaned with diluted ethanol (50%) between sessions.

## 2.3 | Western blot analysis

We used snap-frozen hippocampi (available or remaining) from  $n = 6$ –11 C57Bl6j mice per time point (sham, 72 h, 1 week, and 8 weeks) for the ih and ip KA models and  $n = 6$ –9 J20 mice and relative WT littermates. Western blot was performed as previously described.<sup>20–22</sup> Table S1 provides the list of antibodies used. Representative blots are provided in Figures S1A, S2A, and S3B. Briefly, the

(A) Epileptogenesis

Spontaneous seizures

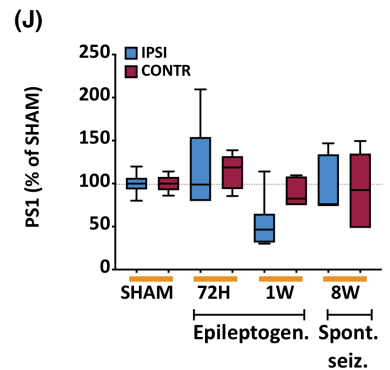
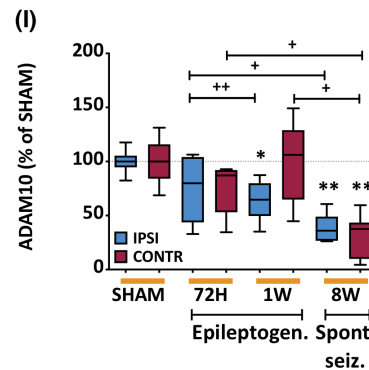
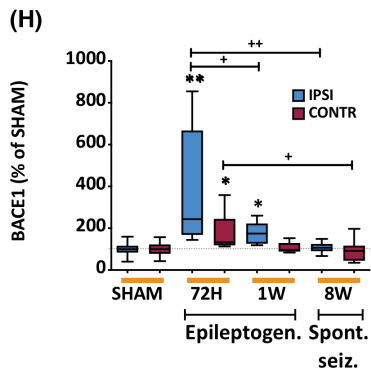
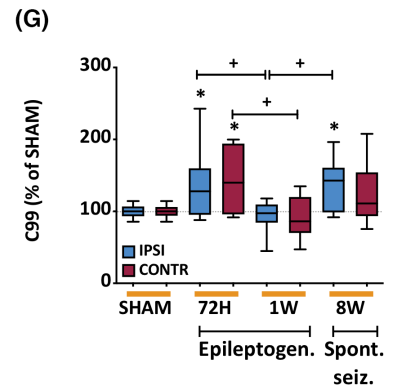
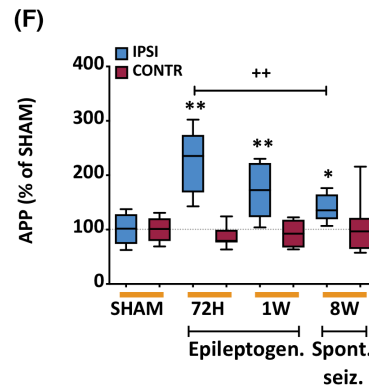
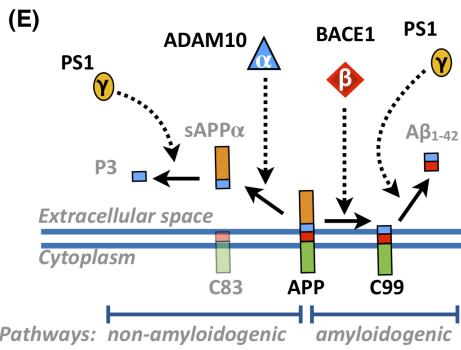
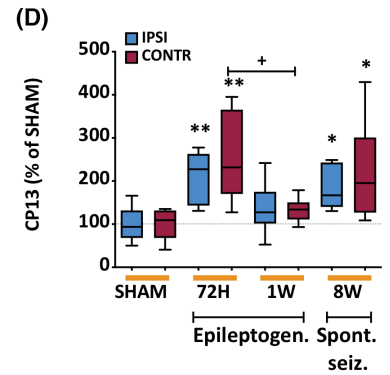
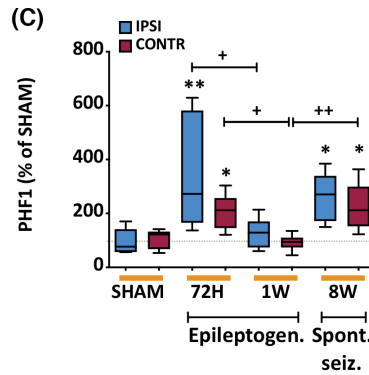
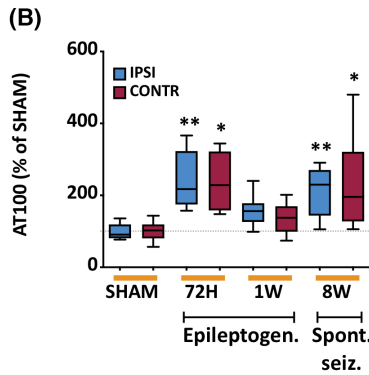
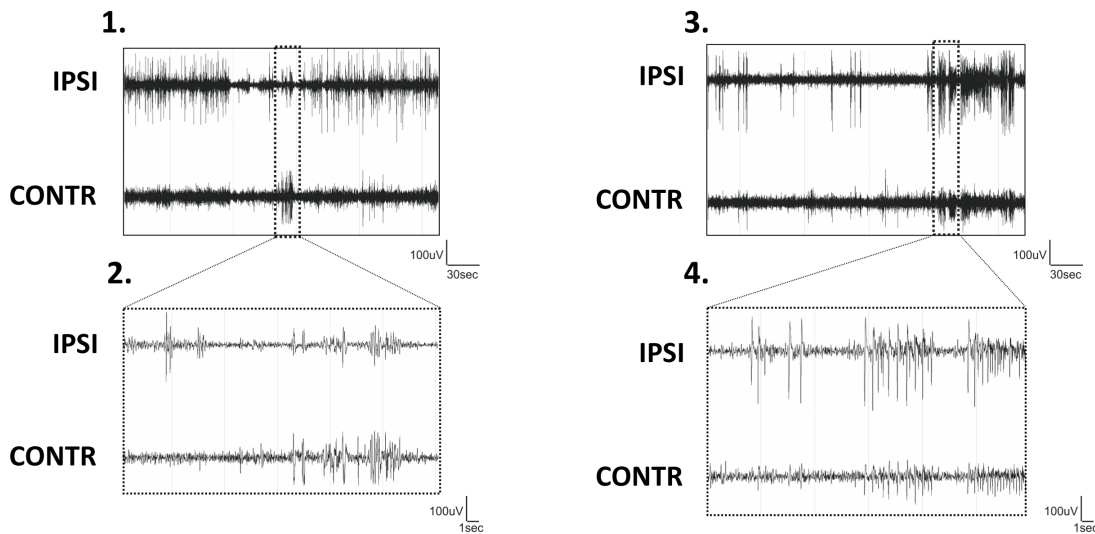


**FIGURE 1** Epileptogenesis and mesial temporal lobe epilepsy (MTLE) elicit persistent tau hyperphosphorylation and amyloidogenic markers in the epileptogenic (ipsilateral [IPSI]) and in seizure propagating (contralateral [CONTR]) hippocampi. (A) Examples of intrahippocampal electroencephalographic recordings during epileptogenesis (72 h; Panels 1 and 2), and spontaneous seizures (8 weeks; Panels 3 and 4) in a model of MTLE. Tau-related and proamyloidogenic markers (E) were evaluated by Western blot in the IPSI and CONTR hippocampi. (B) AT100 (p[T212/S214]tau, 60 kDa), (C) PHF1 (p[S396/S404]tau, 60 kDa), (D) CP13 (p[S202]tau, 60 kDa), (F) APP (120 kDa), (G) C99 (13 kDa), (H) BACE1 ( $\beta$ -secretase, 70 kDa), (I) ADAM10 ( $\alpha$ -secretase, 70 kDa), and (J) PS1 ( $\gamma$ -secretase, 20 kDa) were evaluated in each group and normalized by  $\beta$ -tubulin (55 kDa) or total Tau (TauC, 60kDa). Data are presented as box and whiskers with minimum to maximum and median. Two independent one-way analyses of variance followed by Tukey multiple comparison were performed. IPSI AT100:  $F_{3,28} = 8.59$  ( $p < .001$ ), CONTR AT100:  $F_{3,27} = 5.00$  ( $p < .001$ ), IPSI PHF1:  $F_{3,27} = 7.10$  ( $p < .01$ ), CONTR PHF1:  $F_{3,26} = 9.97$  ( $p < .001$ ), IPSI CP13:  $F_{3,28} = 6.49$  ( $p < .01$ ), CONTR CP13:  $F_{3,27} = 5.62$  ( $p < .01$ ), IPSI APP:  $F_{3,29} = 15.16$  ( $p < .0001$ ), CONTR APP:  $F_{3,31} = .45$  (not significant [ns]), IPSI C99:  $F_{3,36} = 5.87$  ( $p < .01$ ), CONTR C99:  $F_{3,36} = 4.28$  ( $p < .05$ ), IPSI BACE1:  $F_{3,34} = 10.60$  ( $p < .0001$ ), CONTR BACE1:  $F_{3,34} = 4.83$  ( $p < .01$ ), IPSI PS1:  $F_{3,20} = .91$  (ns), CONTR PS1:  $F_{3,20} = .98$  (ns), IPSI ADAM10:  $F_{3,22} = 13.24$  ( $p < .0001$ ), CONTR ADAM10:  $F_{3,22} = 13.28$  ( $p < .0001$ ). Data are expressed as percentage of respective sham mice (intrahippocampal injection of NaCl .9%). \* $p < .05$  and \*\* $p < .01$  versus respective sham hippocampus; + $p < .05$  and ++ $p < .01$  versus selected group

hippocampi were microdissected, weighed, immediately frozen on liquid nitrogen, and stored at  $-20^{\circ}\text{C}$ . Tissues were sonicated in a lysis buffer and centrifuged ( $4^{\circ}\text{C}$ ). Supernatants were collected, and the protein concentration was measured using a bicinchoninic acid assay (BCA) kit (Thermo Fisher Scientific). Sixty micrograms from each sample was used for analysis. Samples were separated in sodium dodecyl sulfate (SDS)–polyacrylamide gel (12%) and transferred to a polyvinylidene difluoride membrane (Merck-Millipore). The membrane was incubated overnight ( $4^{\circ}\text{C}$ ) with the primary antibody, rinsed, and then incubated for 2 h with the appropriate horseradish peroxidase-conjugated secondary antibody. The peroxidase activity was revealed using enhanced chemiluminescence reagents (Luminata-Crescendo, Merck-Millipore). The intensity of peroxidase activity was quantified using ImageJ software (National Institutes of Health).  $\beta$ -Tubulin (or total Tau) was used as a loading control.

## 2.4 | Real-time qPCR

We used available or remaining snap-frozen hippocampi from  $n = 5$ – $8$  C57Bl6j mice per time point (sham, 72 h, 1 week, and 8 weeks) and  $n = 4$  J20 and control littermates. Tissues were suspended in 350  $\mu\text{l}$  RLT Plus buffer (Qiagen) supplemented with 1%  $\beta$ -mercaptoethanol and lysed in a Lysing Matrix D tube into the FastPrep sample preparation system (MP Biomedicals). Tissue lysate was homogenized on QIAshredder columns (Qiagen). Total cellular RNA was extracted using the RNeasy Mini RNA isolation kit (Qiagen), and genomic DNA contamination was removed using the RNase-Free DNase Set (Qiagen). The RNA concentration of each sample was measured with a Nanodrop 2000c spectrophotometer (Thermo Fisher Scientific). Following the manufacturer's instructions, 1  $\mu\text{g}$  of total RNA was reverse-transcribed using random hexamers of the Transcriptor First Strand cDNA Synthesis Kit (Roche). Real-time qPCR was performed using a 5- $\mu\text{l}$  volume of

10 ng cDNA, 500  $\text{nmol}\cdot\text{L}^{-1}$  of forward and reverse primers, and 2.5  $\mu\text{l}$  of SYBR Green PCR Master Mix (Roche) in duplicate. The program ran 45 cycles of denaturation at  $95^{\circ}\text{C}$  for 10 s, annealing at  $60^{\circ}\text{C}$  for 10 s, and elongation at  $72^{\circ}\text{C}$  for 15 s, performed in a LightCycler 480 apparatus (Roche). After amplification, the melting curve was assessed to ensure a single product. Each plate carried serial dilutions of an RNA calibrator to generate a standard curve of the efficiency of the primer during the run. Results were quantified by the comparative  $2\Delta\Delta\text{Ct}$  method. Ct values of the target gene were normalized with the Ct values of the house-keeping gene *GAPDH* (glyceraldehyde 3-phosphate dehydrogenase). Each of the target values is expressed as an  $n$ -fold difference relative to the experimental control. Table S2 provides a list of the primers used.

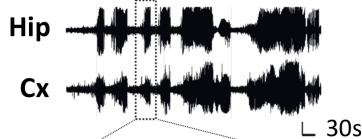
## 2.5 | Corticosterone and soluble $\text{A}\beta_{1-42}$ assays

Blood samples were collected at the time of sacrifice (in BD vacutainer EDTA tubes) and centrifuged at  $4^{\circ}\text{C}$ , and plasma was stored at  $-20^{\circ}\text{C}$ . Corticosterone was measured<sup>20,23</sup> using an enzyme-linked immunosorbent assay (ELISA) kit (ARBOR Assays), and 5  $\mu\text{l}$  of plasma sample was diluted (1:100) with the assay buffer. The assay sensitivity was 17.5  $\text{pg}/\text{ml}$ . The intra- and interassay coefficients were 5.2% and 7.9%, respectively. Amyloid- $\beta$  1–42 ( $\text{A}\beta_{1-42}$ ) peptide was quantified in the soluble fraction of hippocampus homogenates using an ELISA kit (Human  $\text{A}\beta_{42}$  Ultrasensitive ELISA Kit, Invitrogen).<sup>18</sup> Briefly, 2% SDS was added to brain homogenates before ultracentrifugation at 19 600  $\times g$  for 30 min at  $4^{\circ}\text{C}$ . Supernatants obtained were used to quantify soluble fractions of  $\text{A}\beta_{1-42}$  peptides. Results were normalized to protein concentrations calculated using the bicinchoninic acid method (BCA kit, Pierce). The assay sensitivity was 1  $\text{pg}/\text{ml}$ . The intra- and interassay coefficients were 8.6% and 7.5%, respectively.

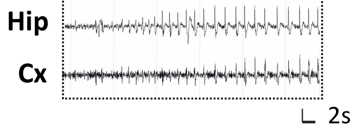
(A)

Generalize SE

1.

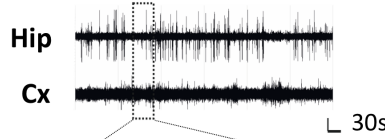


2.

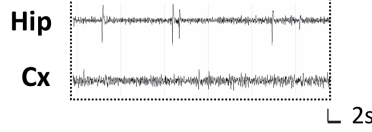


Post-SE 72H

3.

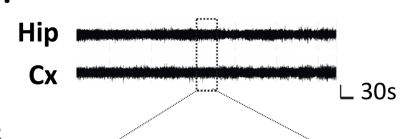


4.

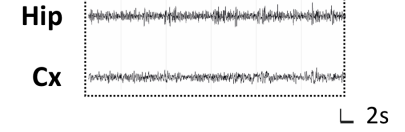


Post-SE 8W

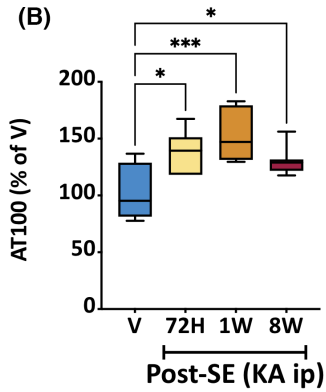
5.



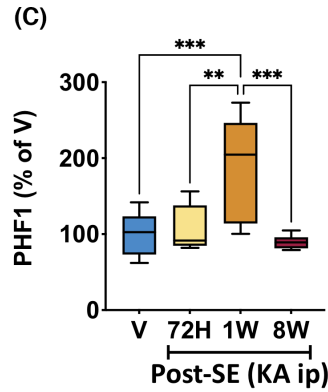
6.



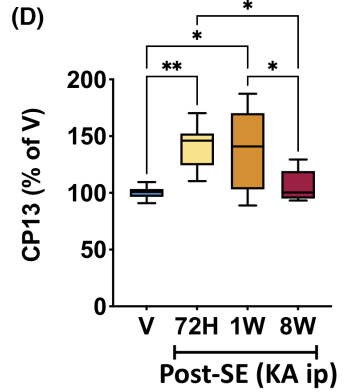
(B)



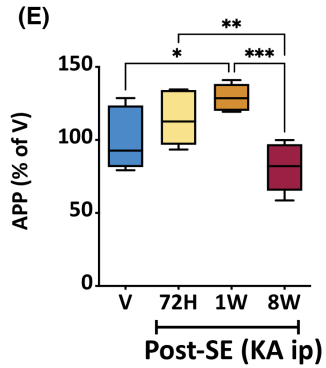
(C)



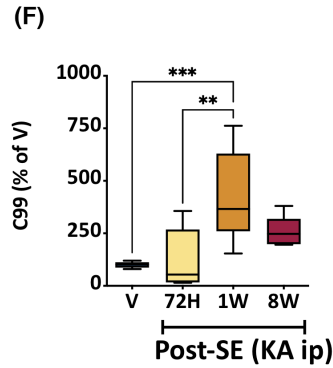
(D)



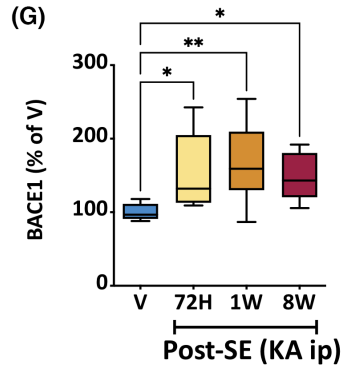
(E)



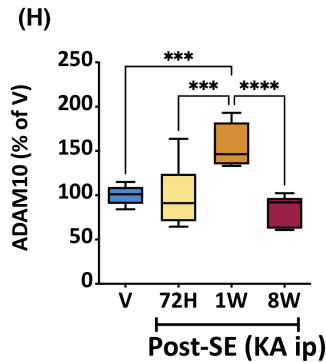
(F)



(G)



(H)



(I)

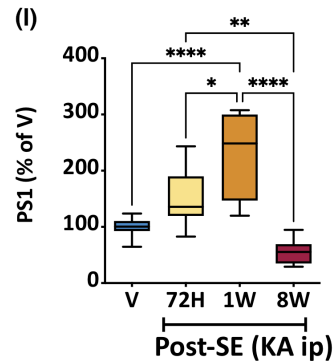


**FIGURE 2** Generalized status epilepticus (SE) elicits time-dependent trajectories of tau-related and amyloidogenic markers in the hippocampus. (A) Examples of intrahippocampal (Hip) and intracortical (Cx) electroencephalographic recordings during SE (Panels 1 and 2), 72 h (Panels 3 and 4), and 8 weeks (Panels 5 and 6) post-SE in the model used (see Figure S4 for spike quantifications over time). Amyloidogenic and tau-related markers were evaluated in the hippocampus by Western blot. Changes in the expression of (B) AT100 (p[T212/S214]tau, 60 kDa), (C) PHF1 (p[S396/S404]tau, 60 kDa), (D) CP13 (p[S202]tau, 60 kDa), (E) APP (120 kDa), (F) C99 (13 kDa), (G) BACE1 ( $\beta$ -secretase, 70 kDa), (H) ADAM10 ( $\alpha$ -secretase, 70 kDa), and (I) PS1 ( $\gamma$ -secretase, 20 kDa) were evaluated in each group and normalized by  $\beta$ -tubulin (55 kDa) or total Tau (TauC, 60kDa). Data are presented as box and whiskers with minimum to maximum and median. A one-way analysis of variance followed by Tukey multiple comparison test was performed. AT100:  $F_{3,25} = 9.04$  ( $p < .001$ ), PHF1:  $F_{3,27} = 10.04$  ( $p < .001$ ), CP13:  $F_{3,25} = 7.44$  ( $p < .001$ ), APP:  $F_{3,24} = 9.57$  ( $p < .001$ ), C99:  $F_{3,22} = 8.94$  ( $p < .001$ ), BACE1:  $F_{3,33} = 5.70$  ( $p < .01$ ), ADAM10:  $F_{3,29} = 12.08$  ( $p < .001$ ), PS1:  $F_{3,27} = 17.48$  ( $p < .001$ ). Data are expressed as percentage of mice treated with vehicle (V; .9% NaCl). \* $p < .05$ , \*\* $p < .01$ , \*\*\* $p < .001$ , \*\*\*\* $p < .0001$  versus selected group. ip, intraperitoneal; KA, kainic acid

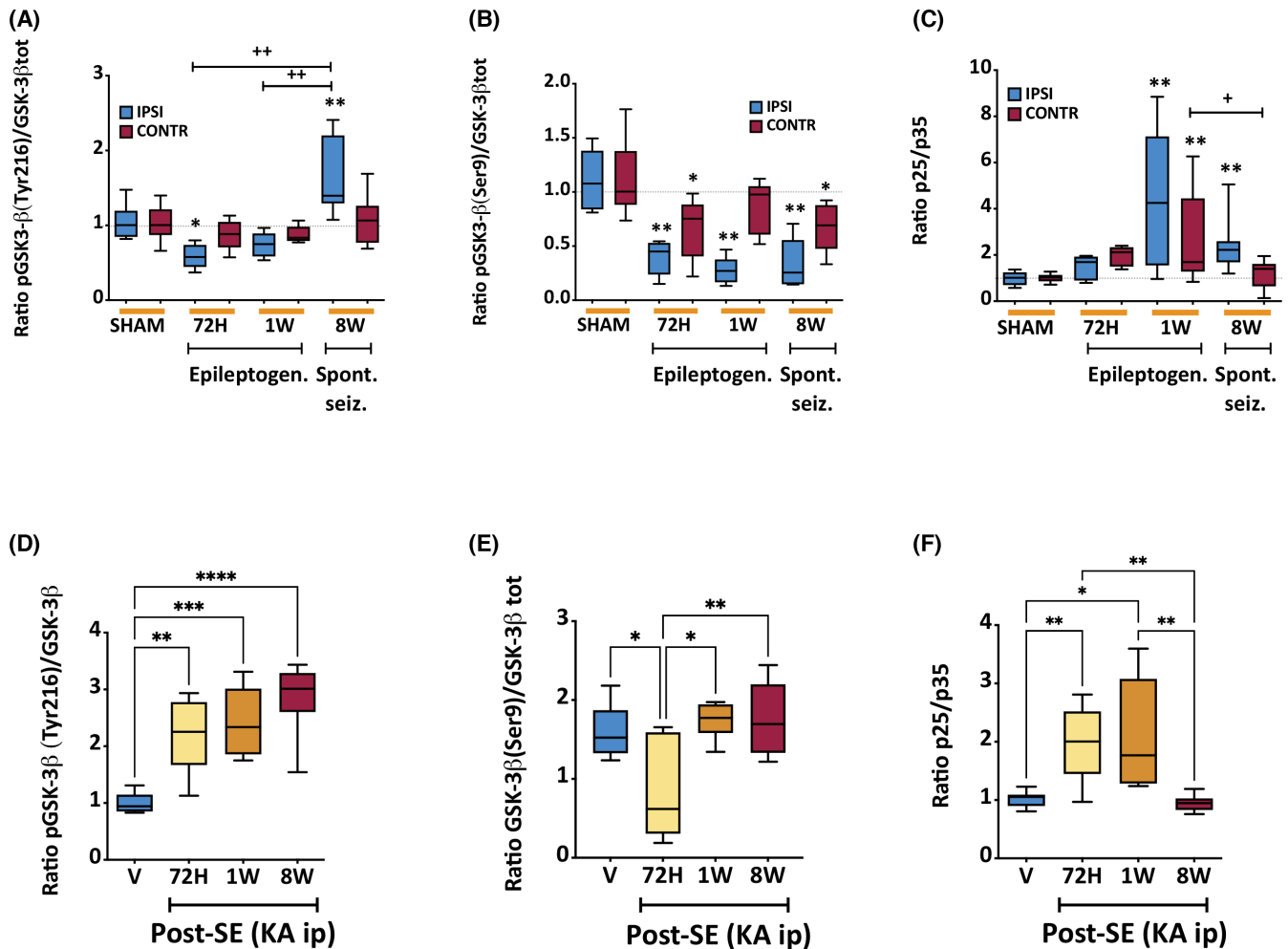


**FIGURE 3** Hippocampal expression of tau-related kinases during mesial temporal lobe epilepsy (MTLE) and after a generalized status epilepticus (SE). Changes in the expression of (A,D) p[Y216]GSK-3 $\beta$ /GSK-3 $\beta$  (active form, 46 kDa), (B,E) p[S9]GSK-3 $\beta$ /GSK-3 $\beta$  (inactive form, 46 kDa), and (C,F) p25/p35 (25/35 kDa) were evaluated in each group and normalized by  $\beta$ -tubulin (55 kDa). Data are presented as box and whiskers with minimum to maximum and median. For MTLE animals, two independent one-way analyses of variance (ANOVA) followed by Tukey multiple comparison were performed for ipsilateral (IPSI) and contralateral (CONTR) samples. IPSI p[Y216]GSK-3 $\beta$ /GSK-3 $\beta$ :  $F_{3,28} = 17.67$  ( $p < .001$ ), CONTR p[Y216]GSK-3 $\beta$ /GSK-3 $\beta$ :  $F_{3,28} = 1.31$  (not significant), IPSI p[S9]GSK-3 $\beta$ /GSK-3 $\beta$ :  $F_{3,18} = 18.26$  ( $p < .001$ ), CONTR p[S9]GSK-3 $\beta$ /GSK-3 $\beta$ :  $F_{3,19} = 3.531$  ( $p < .05$ ), IPSI p25/p35:  $F_{3,31} = 8.25$  ( $p < .001$ ), CONTR p25/p35:  $F_{3,31} = 5.31$  ( $p < .01$ ). Data are expressed as percentage of respective sham mice (intrahippocampal injection of NaCl .9%). \* $p < .05$  and \*\* $p < .01$  versus respective sham hippocampus; + $p < .05$  and ++ $p < .01$  versus selected group. For SE animals, a one-way ANOVA followed by Tukey multiple comparison test was performed: p[Y216]GSK-3 $\beta$ /GSK-3 $\beta$ :  $F_{3,25} = 17.35$  ( $p < .0001$ ), p[S9]GSK-3 $\beta$ /GSK-3 $\beta$ :  $F_{3,22} = 8.08$  ( $p < .001$ ), P25/P35:  $F_{3,31} = 11.74$  ( $p < .0001$ ). Data are expressed as percentage of mice treated with vehicle (V; .9% NaCl). \* $p < .05$ , \*\* $p < .01$ , \*\*\* $p < .001$ , \*\*\*\* $p < .0001$  versus selected group



## 2.6 | Statistical analysis

Data are presented as box and whiskers (minimum to maximum), including the median value. Before each analysis of variance, the Gaussian distribution was evaluated and validated by a Kolmogorov–Smirnov test (GraphPad Prism 9.0). Nonparametric tests were used (Mann–Whitney and Dunn) when the distribution was not normal. Two- or one-way analysis of variance followed by Tukey multiple comparison tests were used for the normally distributed data set.  $p < .05$  was considered significant. The number of animals in each group and statistical details are indicated in the figure legends. Statistical power analysis was calculated using G\*Power.

## 3 | RESULTS

### 3.1 | Epileptogenesis and MTLE seizures are associated with persistent overexpression of AD-relevant markers in epileptogenic and seizure propagating zones

Using the MTLE model, we tested the hypothesis that seizure progression triggers the expression of AD-relevant markers. We examined AT100, PHF-1, and CP13, indicating phosphorylation sites typical of pathological tau in the early and advanced stages of AD.<sup>24</sup> These markers were overexpressed in the ipsilateral hippocampus during epileptogenesis (72 h to 1 week) and spontaneous seizures (8 weeks; Figure 1B–D). AT100, PHF-1, and CP13 levels were also increased in the contralateral hippocampus (Figure 1B–D), a nonlesional zone where EEG seizures propagate (Figure 1A).<sup>8</sup> Furthermore, the two main kinases Cdk5 and GSK-3 $\beta$ , involved in the pathological phosphorylation of tau, were activated. Specifically, p25/p35 ratio (indicating Cdk5 activity) increased during epileptogenesis (from 1 week; Figure 3C). The GSK-3 $\beta$  was activated, as shown by a sustained GSK-3 $\beta$ (Ser9) decrease and GSK-3 $\beta$ (Tyr216) increase during spontaneous seizures (8 weeks; Figure 3A,B). Altogether, these results support a mechanism for pathological tau hyperphosphorylation in the lesional epileptogenic and nonlesional seizure propagating zones over time.

The subsequent analysis of proamyloidogenic markers (Figure 1E) showed the overexpression of APP (amyloid precursor protein; Figure 1F), C99 (precursor of  $\beta$ -amyloid peptides; Figure 1G), and BACE1 ( $\beta$ -secretase involved in the amyloidogenic pathway; Figure 1H) in the ipsilateral epileptogenic hippocampus. BACE1 expression returned to control levels at 8 weeks (Figure 1H). Furthermore,

ADAM10 ( $\alpha$ -secretase involved in the nonamyloidogenic pathway; Figure 1E) was decreased during seizure progression (Figure 1I), whereas PS1 (presenilin, the  $\gamma$ -secretase involved in the maturation of APP fragments) levels were unchanged (Figure 1J). In the contralateral seizure propagating hippocampus, the proamyloidogenic changes were restricted to C99, and BACE1 increased specifically at 72 post-SE (Figure 1G,H), whereas ADAM10 was decreased only at 8 weeks (Figure 1I).

Next, we asked whether pathological analogies exist in MTLE and an experimental AD model, the J20 mice. We specifically cross-compared advanced stages of disease in the MTLE (spontaneous seizures) and J20 models (9 months old).<sup>18</sup> The hippocampi displayed a similar tau hyperphosphorylation signature (PHF1, CP13, pGSK-3 $\beta$ [Tyr216], Cdk5-p25; Figure 5C,H). By contrast, the expression of amyloidogenic markers (BACE1 and ADAM10; Figure 5A,B), postsynaptic marker PSD95, and presynaptic marker synaptotagmin (SYN) were dissimilar (Figure 5C,D). These results indicate that MTLE progression causes tau hyperphosphorylation, with certain elements relevant to an AD setting, in the epileptogenic and seizure propagating hippocampi (Figure 7C,D).

### 3.2 | The overexpression of AD-relevant markers after a generalized SE episode is predominantly transient

Generalized SE can represent a clinical risk factor for unfavorable neurological sequelae.<sup>25</sup> Here, we tested the hypothesis that an SE episode is sufficient to trigger the expression of proamyloidogenic and tau-related markers. Figure 2A shows an EEG example of SE after ip KA injection, indicating the absence of epileptogenesis (quantified in Figure S4), as previously recognized.<sup>13</sup> This model presented tau hyperphosphorylation on AT100, PHF1, and CP13 epitopes (Figure 2B–D) at 72 h and 1 week post-SE, with PHF1 and CP13 returning to control levels at 8 weeks (Figure 2C,D). Tau hyperphosphorylation was associated with the activation of GSK-3 $\beta$  and Cdk5-p25 kinases. In particular, pGSK-3 $\beta$ (Tyr216) (the active form; Figure 3D) and p25/p35 (Figure 3F) were increased, whereas the inactive form pGSK-3 $\beta$ (Ser9) was unchanged or decreased over time (Figure 3E). Additionally, SE caused the expression of amyloidogenic markers APP (Figure 2E), C99 (Figure 2F), BACE1 (Figure 2G), ADAM10 (Figure 2H), and PS1 (Figure 2I) in the hippocampus, however, not enduring long-term except for BACE1. Finally, by cross-comparing the SE and MTLE settings, we qualitatively outlined the AD-relevant markers that depend on epileptogenesis, the presence of a tissue lesion, and seizure propagation (Figure 7B–D).

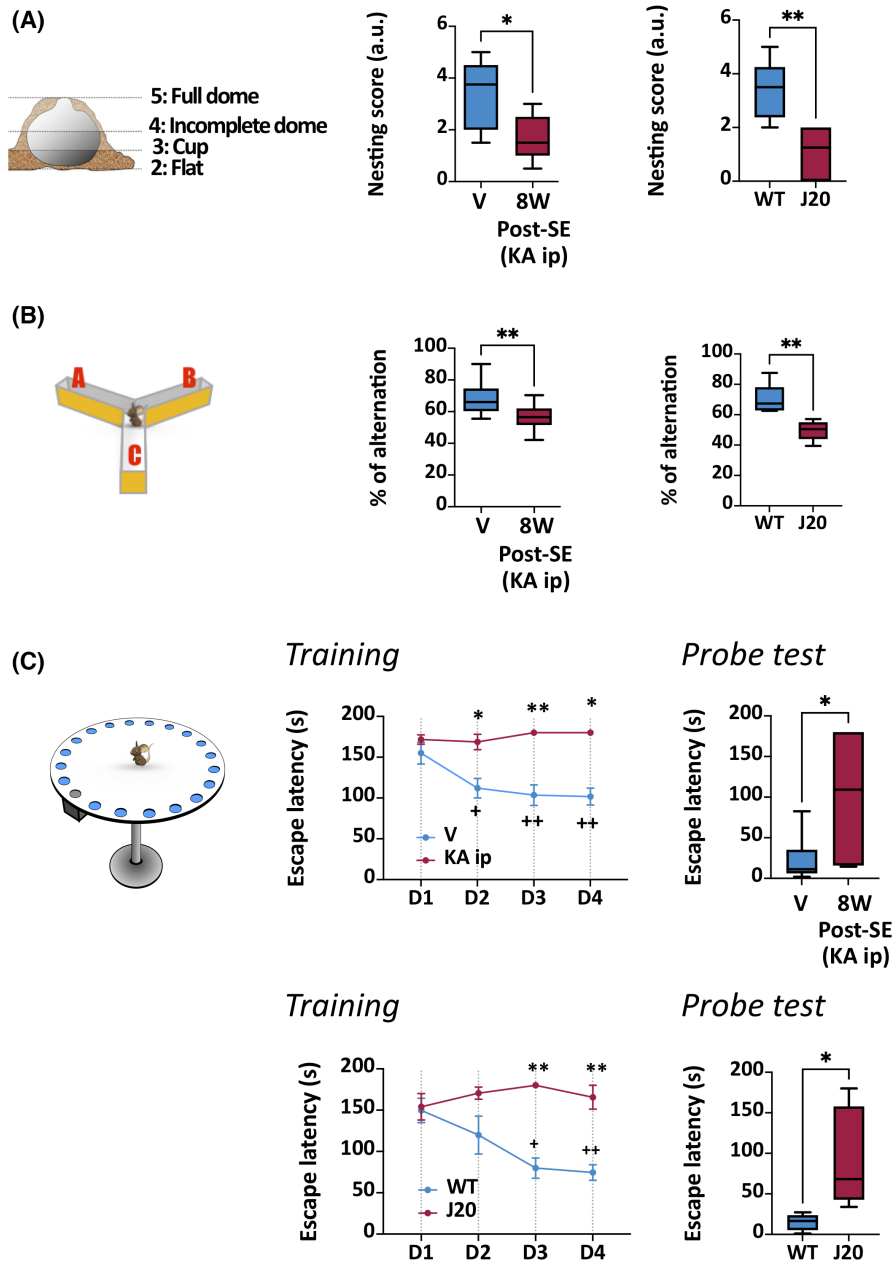
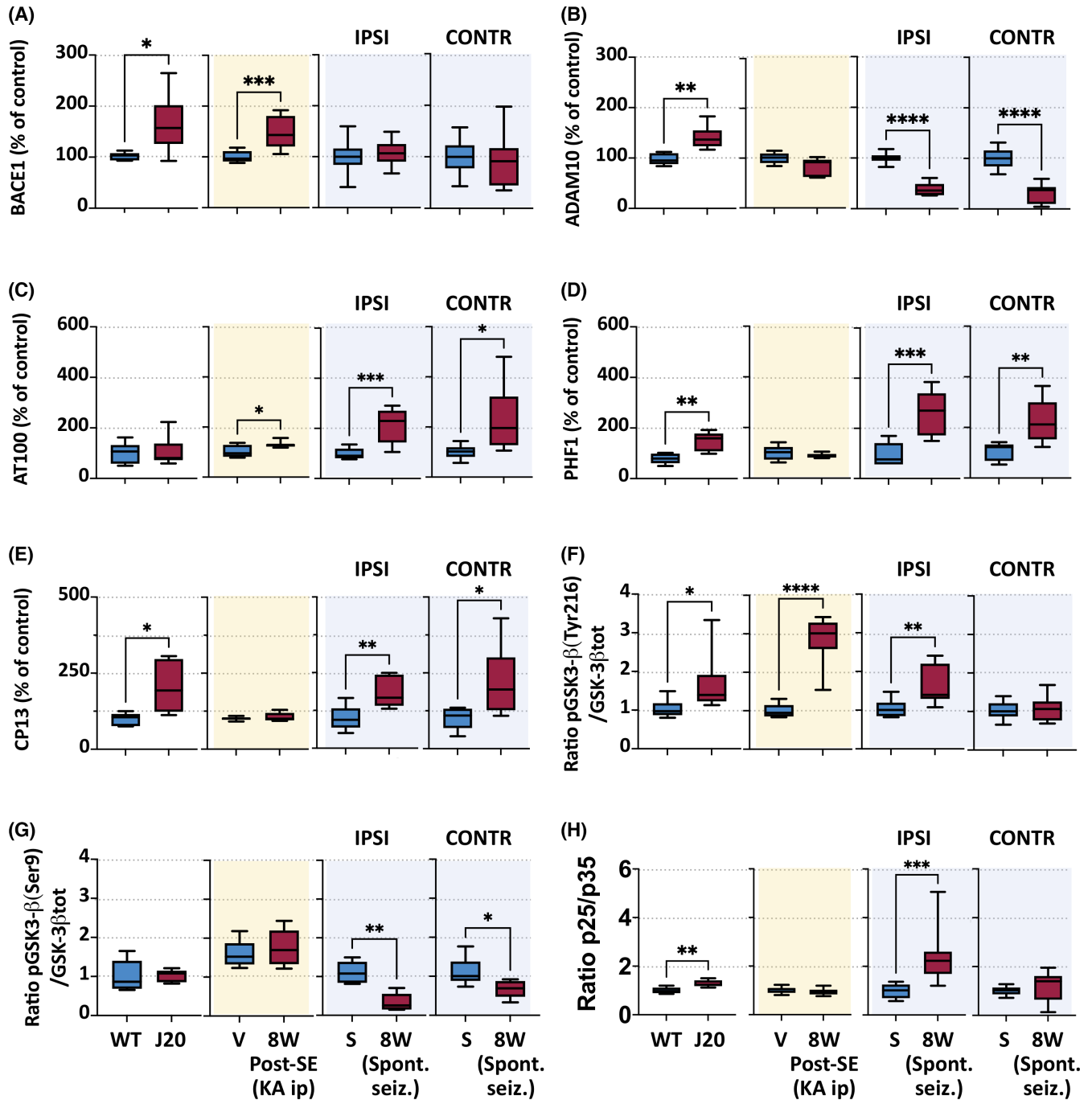


**FIGURE 4** Cross-comparisons of long-term cognitive and memory deficits in post-status epilepticus (SE) and J20 models. (A) The nest scoring test evaluated general welfare behavior. For SE animals, a nonparametric Mann–Whitney test was performed ( $p < .05$ ), whereas for J20 mice, an unpaired  $t$ -test was used ( $p < .01$ ). \* $p < .05$ , \*\* $p < .01$  versus respective control. (B) The Y-maze test evaluated spontaneous working memory. The number of arm entries and the number of triads are recorded to calculate the percentage of alternations. For SE animals and J20 mice, an unpaired  $t$ -test was performed ( $p < .001$  and  $p < .01$ , respectively). \*\* $p < .01$  versus respective control. (C) Learning and long-term memory were evaluated in the Barnes maze test. Training curves: two-way analysis of variance followed by Tukey multiple comparison test was performed. For SE animals:  $F_{1,44} = 65.81$  for group ( $p < .0001$ ),  $F_{3,44} = 2.53$  for time (not significant [ns]), and  $F_{3,44} = 4.15$  for interaction ( $p < .05$ ). For J20 animals:  $F_{1,36} = 34.40$  for group ( $p < .0001$ ),  $F_{3,36} = 2.05$  for day (ns), and  $F_{3,36} = 4.73$  for interaction ( $p < .01$ ). Data are expressed as the mean latency (s) each day for each animal to find the escape box. \* $p < .05$  and \*\* $p < .01$  versus the respective day of the respective control group. + $p < .05$  and ++ $p < .01$  versus Day 1 (D1). Probe test graph: For SE animals, a nonparametric Mann–Whitney test was performed ( $p < .05$ ), whereas for J20 mice, a paired  $t$ -test was performed ( $p < .05$ ). Data are expressed as the mean latency (s) for each animal to find the escape whole. \* $p < .05$  versus respective control. All results are presented as box and whiskers with minimum to maximum and median, except for training curves, where results are presented as mean  $\pm$  SEM. ip, intraperitoneal; KA, kainic acid; V, vehicle



Next, we examined whether the post-SE molecular modifications were associated with long-lasting functional consequences. Behavioral outcome was also compared to the J20 model. The adopted generalized SE model does not cause recurrent seizures, allowing uncomplicated behavioural testing. Disrupted nest-building capabilities indicated well-being deficits 8 weeks post-SE,<sup>26</sup> similar to J20 mice with A $\beta$  pathology (Figure 4A).<sup>18</sup> We discovered short-term (Y-maze) and long-term (Barnes test) spatial memory deficits (Figure 4B,C). These changes were associated with apoptosis (Casp-3, Table S3) and synaptic deficits (PSD95 and SYN; Figure S2B,C), similarly to

J20 mice (Figure S3C,D). We also found GSK3- $\beta$  (Figure 5F) and BACE1 (Figure 5A) increase in the two models. Nevertheless, considerable modifications existed as in J20 mice, and not post-SE, PHF1 (Figure 5D) and CP13 (Figure 5E) were increased, and AT100 was unchanged (Figure 5C). The expression pattern of kinase Cdk5-p25 was dissimilar in the two settings (Figure 5H). Figure 7A,B graphically illustrates these distinct trajectories. In summary, a generalized SE triggers a time-dependent, primarily transient, induction of specific AD-relevant markers. This is associated with long-term well-being and memory deficits, consistent with hippocampal dysfunction.

**FIGURE 5** Cross-comparisons of long-term pathological trajectories in post-status epilepticus (SE), mesial temporal lobe epilepsy (MTLE), and J20 models. Variations of pertinent proamyloidogenic and tau-related markers were evaluated by Western blot in the hippocampus of 9-month-old J20 mice (left panel), and compared with generalized SE (second panel in light yellow) and MTLE animals (right panels in light blue, in the ipsilateral [IPSI] and contralateral [CONTR] hippocampi), 8 weeks after kainic acid (KA) injections. (A) BACE1 ( $\beta$ -secretase, 70 kDa), (B) ADAM10 ( $\alpha$ -secretase, 70 kDa), (C) AT100 (p[T212/S214]tau, 60 kDa), (D) PHF1 (p[S396/S404]tau, 60 kDa), (E) CP13 (p[S202]tau, 60 kDa), (F) p[Y216]GSK-3 $\beta$ /GSK-3 $\beta$  (active form, 46 kDa), (G) p[S9]GSK-3 $\beta$ /GSK-3 $\beta$  (inactive form, 46 kDa), and (H) p25/p35 (25/35 kDa) were evaluated in each group and normalized by  $\beta$ -tubulin (55 kDa) or total Tau (TauC, 60kDa). Data are presented as box and whiskers with minimum to maximum and median. For J20 mice, unpaired *t*-tests were performed: BACE1 ( $p < .05$ ), ADAM10 ( $p < .001$ ), AT100 (not significant [ns]), PHF1 ( $p < .01$ ), CP13 ( $p < .05$ ), p[Y216]GSK-3 $\beta$ /GSK-3 $\beta$  ( $p < .05$ ), p[S9]GSK-3 $\beta$ /GSK-3 $\beta$  (ns), p25/p35 ( $p < .01$ ). Data are expressed as percentage of wild-type (WT) mice. For SE animals, unpaired *t*-tests were performed: BACE1 ( $p < .001$ ), ADAM10 (ns), AT100 ( $p < .05$ ), PHF1 (ns), CP13 (ns), p[Y216]GSK-3 $\beta$ /GSK-3 $\beta$  ( $p < .0001$ ), p[S9]GSK-3 $\beta$ /GSK-3 $\beta$  (ns), p25/p35 (ns). Data are expressed as percentage of mice treated with vehicle (V; .9% NaCl). For MTLE animals, two independent unpaired *t*-tests were performed for IPSI and CONTR samples: IPSI BACE1 (ns), CONTR BACE1 (ns), IPSI ADAM10 ( $p < .0001$ ), CONTR ADAM10 ( $p < .0001$ ), IPSI AT100 ( $p < .001$ ), CONTR AT100 ( $p < .05$ ), IPSI PHF1 ( $p < .001$ ), CONTR PHF1 ( $p < .01$ ), IPSI CP13 ( $p < .01$ ), CONTR CP13 ( $p < .05$ ), IPSI p[Y216]GSK-3 $\beta$ /GSK-3 $\beta$  ( $p < .01$ ), CONTR p[Y216]GSK-3 $\beta$ /GSK-3 $\beta$  (ns), IPSI p[S9]GSK-3 $\beta$ /GSK-3 $\beta$  ( $p < .01$ ), CONTR p[S9]GSK-3 $\beta$ /GSK-3 $\beta$  ( $p < .05$ ), IPSI p25/p35 ( $p < .001$ ), CONTR p25/p35 (ns). Data are expressed as percentage of respective sham hippocampus (intrahippocampal injection of NaCl .9%). \* $p < .05$ , \*\* $p < .01$ , \*\*\* $p < .001$ , \*\*\*\* $p < .0001$  versus respective control mice. ip, intraperitoneal

### 3.3 | Divergent patterns of neuroinflammation reciprocate AD-relevant markers during MTLE and after a generalized SE

Finally, we asked how inflammation associates with the outlined pathological patterns in the two seizure models.<sup>27</sup> We focused on the equilibrium between pro-inflammatory glia activation and cytokine/chemokine release and the anti-inflammatory activity of the glucocorticoid receptor (GR).<sup>11,20,23</sup> In the MTLE model, we report a stable increase of GFAP and Iba1 (Figure S1D,E and Figure 6A,B) with no participation of an endogenous anti-inflammatory response, as indicated by the decreased GR phosphorylation (pGR/GR) long-term in the ipsilateral epileptogenic and contralateral seizure propagating hippocampi (Figure S1F and Figure 6C), and no variation of corticosterone levels as we previously reported.<sup>11</sup> By contrast, after a generalized SE episode, the increase in GFAP, Iba1 (Figure S2D,E), and transcript levels of soluble cytokines and chemokines (IL-1 $\beta$ , TNF- $\alpha$ , CCL12; Table S3) was transient (72 h to 1 week). This inflammatory response was paralleled and temporally exceeded by GR activation, with increased hippocampal pGR/GR ratio and corticosterone plasma levels (Figure 6C,D and Figure S2F,G), suggesting an enduring anti-inflammatory response. These results indicate that, specifically in MTLE, tau hyperphosphorylation is associated with inflammation or inadequate anti-inflammatory regulation in the epileptogenic and seizure propagating hippocampi. Interestingly, the inflammatory pattern observed in MTLE was similar to the J20 model (GFAP and Iba1; Figure 6A,B), along with a time-dependent deficit of the GR system (Figure 6C).

## 4 | DISCUSSION

Here, we studied the role of experimental seizures in triggering tau hyperphosphorylation and amyloidogenic makers over time, regionally, and with intersections to neuroinflammation. We reported that (1) MTLE is associated with time-persistent tau hyperphosphorylation, in the lesional epileptogenic and the contralateral, non-lesional, seizure propagating hippocampi; (2) a generalized SE elicited mostly transient amyloidogenic and tau hyperphosphorylation signatures; (3) in MTLE, inflammation offsets an endogenous anti-inflammatory mechanism, possibly contributing to the enduring tau hyperphosphorylation; (4) the neurodegenerative pathways in MTLE share elements of similarity with J20 mice, an AD-relevant model.<sup>7,28,29</sup> Defining links between epileptogenic and AD-like trajectories is clinically relevant, and the presented results deepen our knowledge of the neurodegenerative-promoting effect of seizures.<sup>3,4</sup>

### 4.1 | AD-relevant markers in experimental MTLE and implication of nonlesional seizure propagating zones

The use of a model of MTLE<sup>8-10,13,14</sup> has allowed us to examine how hyperexcitable networks in vivo provoke AD-relevant pathological modifications. The reported expression of specific tau-related and amyloidogenic players directly integrates with the neuroinflammatory dynamics in the epileptogenic hippocampus.<sup>8-10,30</sup> Importantly, existing evidence showed learning and memory deficits in the MTLE setting,<sup>13,31,32</sup> an outcome consistent with the patterns of AD-relevant markers outlined here. Our

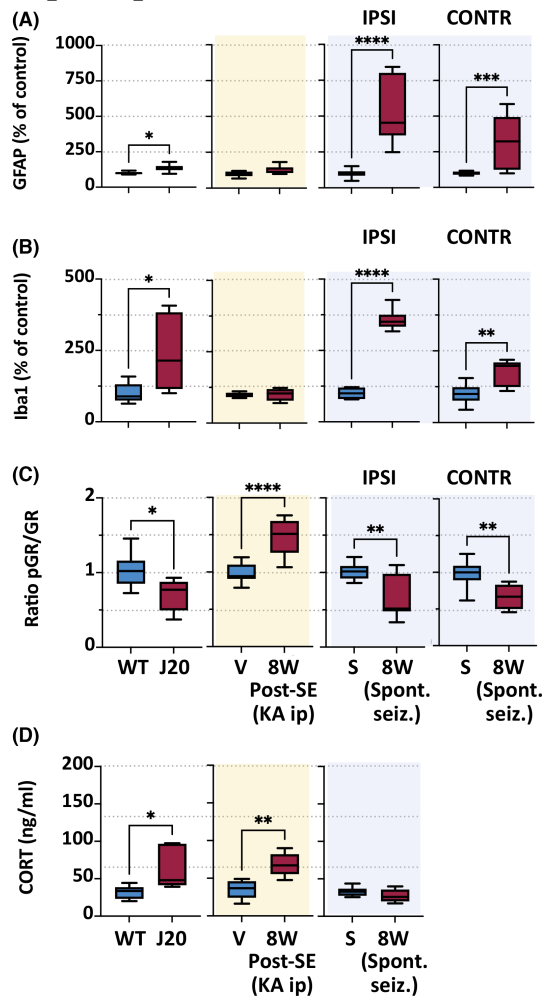
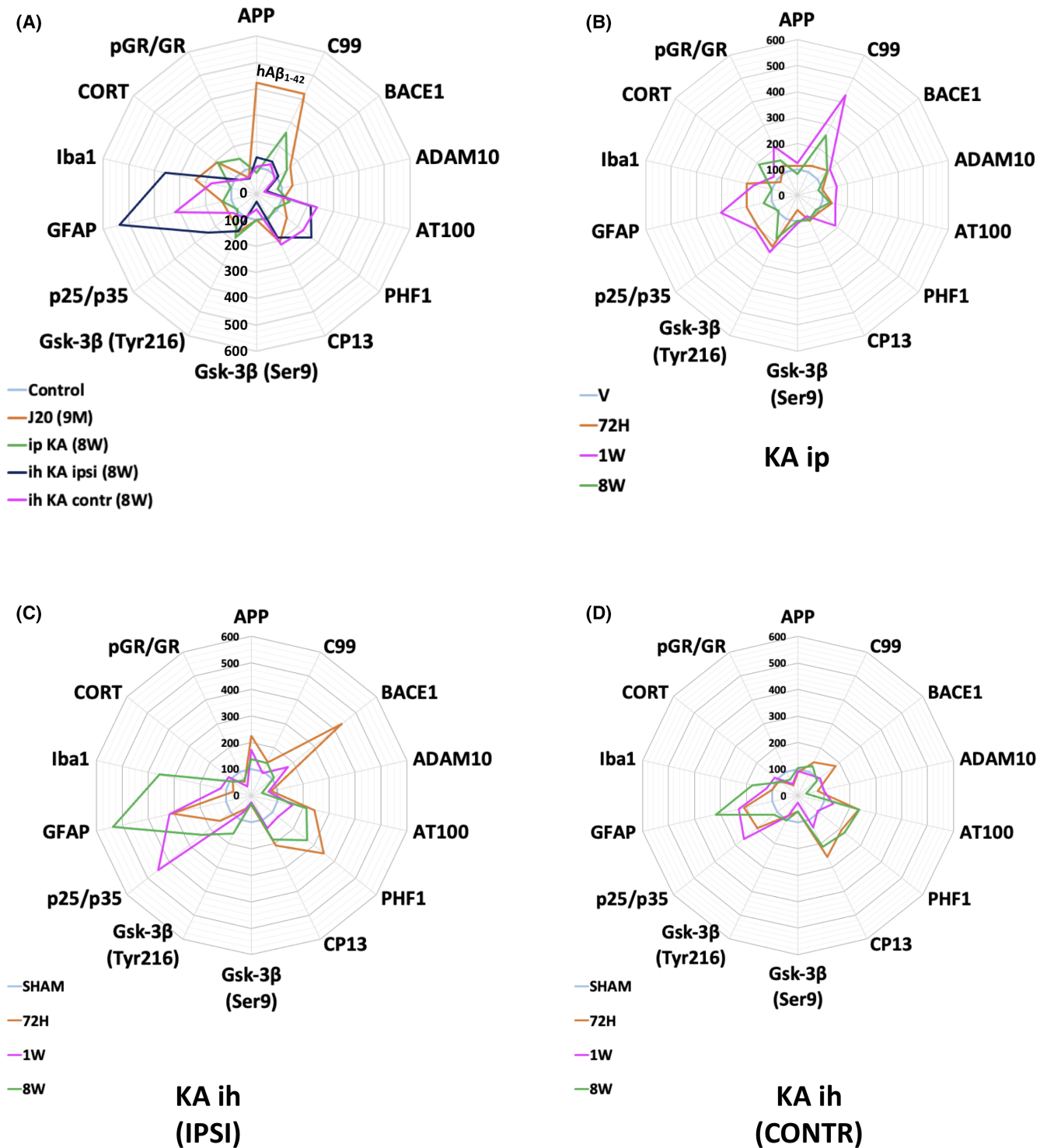


**FIGURE 6** Patterns of hippocampal inflammatory markers in post-status epilepticus (SE), mesial temporal lobe epilepsy (MTLE), and J20 models. (A–C) Variations of hippocampal pro- and anti-inflammatory markers were evaluated by Western blot in the hippocampus of 9-month-old J20 mice (left panel), and compared with generalized SE (second panel in light yellow) and MTLE animals (right panels in light blue, in the ipsilateral (IPSE) and contralateral (CONTR) hippocampi), 8-weeks after kainic acid (KA) injections. (A) GFAP (astrocytes activation, 50 kDa), (B) Iba1 (microglia, 19 kDa), and (C) p[S211]GR/GR (active form of glucocorticoid receptor [GR], 95 kDa) were evaluated in each group and normalized by  $\beta$ -tubulin (55 kDa). Data are presented as box and whiskers with minimum to maximum and median. For J20 mice, unpaired *t*-tests were performed: GFAP ( $p < .05$ ), Iba1 ( $p < .05$ ), ratio p[S211]GR/GR ( $p < .05$ ). Data are expressed as percentage of wild-type (WT) mice. For SE animals, unpaired *t*-tests were performed: GFAP (not significant [ns]), Iba1 (ns), ratio p[S211]GR/GR ( $p < .0001$ ). Data are expressed as percentage of mice treated with vehicle (V; 9% NaCl). For MTLE animals, two independent unpaired *t*-tests were performed for IPSE and CONTR samples: IPSE GFAP ( $p < .0001$ ), CONTR GFAP ( $p < .001$ ), IPSE Iba1 ( $p < .0001$ ), CONTR Iba1 ( $p < .01$ ), IPSE p[S211]GR/GR ( $p < .01$ ), CONTR p[S211]GR/GR ( $p < .01$ ). Data are expressed as percentage of respective sham (S) hippocampus (intra-hippocampal injection of NaCl 9%). \* $p < .05$ , \*\* $p < .01$ , \*\*\* $p < .001$  and \*\*\*\* $p < .0001$  versus respective control. (D) Plasma concentrations of corticosterone (CORT) were determined by enzyme-linked immunosorbent assay and expressed as ng/ml. Data are presented as box and whiskers with minimum to maximum and median. For J20 mice (left panel), intraperitoneal (ip) kainic acid (KA) animals (light yellow panel), and for intra-hippocampal KA animals (light blue panel), unpaired *t*-tests were performed (\* $p < .05$ , \*\* $p < .01$  and ns, respectively)

findings, showing tau hyperphosphorylation, are also consistent with the previously identified modifications in human MTLE brain specimens.<sup>1–4</sup> Of interest, an association between seizures and neurodegenerative pathways is supported by the increased tau and hyperphosphorylated tau levels in the cerebrospinal fluid of subjects with focal or convulsive seizures.<sup>33,34</sup>

Here, we reported tau hyperphosphorylation in the contralateral MTLE hippocampi (Figures 1 and 7C,D). These data support the notion that a seizure propagating zone can carry molecular-level pathological elements even when devoid of lesion. The latter is in accordance with our previous imaging study, indicating distinct

**FIGURE 7** Qualitative comparisons and spatiotemporal trajectories of Alzheimer's disease-relevant and inflammatory markers in mesial temporal lobe epilepsy (MTLE), status epilepticus (SE), and J20 models. (A) Radar chart displaying amyloidogenic pathway (APP, C99, BACE1, ADAM10, specifically for J20 mice), tau hyperphosphorylation (AT100, PHF1, CP13), tau-related kinase (p[Y216]GSK-3 $\beta$ , p[S9]GSK-3 $\beta$ , p25/p35), and pro- and anti-inflammatory marker (GFAP, Iba1, plasma corticosterone [CORT], and pGR/GR) profiles in each experimental model (control, 9-month-old J20 mice, SE, and MTLE 8 weeks after kainic acid [KA] injections). (B) Radar chart displaying amyloidogenic pathway (APP, C99, BACE1, ADAM10), tau hyperphosphorylation (AT100, PHF1, CP13), tau-related kinase (p[Y216]GSK-3 $\beta$ , p[S9]GSK-3 $\beta$ , p25/p35), and pro- and anti-inflammatory marker (GFAP, Iba1, plasma CORT, pGR/GR) profiles in the generalized SE model induced by intraperitoneal (ip) injection of KA (vehicle [V], and 72 h [72H], 1 week [1W], and 8 weeks [8W] post-SE). (C) Radar chart displaying amyloidogenic pathway (APP, C99, BACE1, ADAM10), tau hyperphosphorylation (AT100, PHF1, CP13), tau-related kinase (p[Y216]GSK-3 $\beta$ , p[S9]GSK-3 $\beta$ , p25/p35), and pro- and anti-inflammatory marker (GFAP, Iba1, plasma CORT, pGR/GR) profiles in the ipsilateral (IPSE) hippocampus (intra-hippocampal [ih] KA) of the MTLE model (sham, epileptogenesis 72 h, 1 week, and spontaneous seizures 8 weeks after KA injections). (D) Radar chart displaying amyloidogenic pathway (APP, C99, BACE1, ADAM10), tau hyperphosphorylation (AT100, PHF1, CP13), tau-related kinase (p[Y216]GSK-3 $\beta$ , p[S9]GSK-3 $\beta$ , p25/p35), and pro- and anti-inflammatory marker (GFAP, Iba1, plasma CORT, pGR/GR) profiles in the contralateral (CONTR) hippocampus (nonlesional) of the MTLE model (sham, and 72 h, 1 week, and 8 weeks after KA injections). All data are expressed as percentage of respective control animals



pathological modifications of apparent diffusion coefficient, blood volume fractions, and blood-brain barrier permeability in seizure propagating areas with no sclerosis. Collectively, these data, obtained in the MTLE model, point to a regional overlap between MRI-mapped cerebrovascular dysfunction<sup>8</sup> and tau hyperphosphorylation markers (Figure 1). These results are coherent with the evidence showing vascular dysfunction as an element favoring or sustaining neurodegenerative modifications

and neurological sequel.<sup>35</sup> Because the two hippocampi are strongly interconnected through the ventral commissure, another plausible explanation is that phospho-tau spreads transynaptically, enhanced by neuronal hyperactivity, as previously reported.<sup>36</sup> In general, defining the modalities by which experimental seizures promote molecular imprints that topographically extend beyond the epileptogenic zone could be relevant to clinical cases of complex seizure networks, focal cortical dysplasias, and

MTLE. This knowledge may apply to surgical scenarios where the nonresected brain areas could harbor or contribute to comorbidities postsurgery, contingent to seizures.

## 4.2 | Generalized SE: Risk factor for specific tau and amyloidogenic-related physiological adaptations?

A generalized SE episode can constitute a risk factor for adverse neurophysiological sequelae.<sup>25,37</sup> The clinical relevance is high, considering that SE can be provoked by a plethora of acute injuries such as head trauma and stroke. Although neuronal cell damage or loss following generalized SE is well documented,<sup>13,25,37,38</sup> the amyloidogenic and tau-related trajectories have been incompletely studied. Previously, increased BACE1 expression was reported 48 h after pilocarpine-induced SE,<sup>39</sup> modification of tau hyperphosphorylation occurred within hours after intraperitoneal KA,<sup>40</sup> and the production of A $\beta$ -related peptide was enhanced 12 days after KA.<sup>41</sup> Furthermore, tau hyperphosphorylation was reported in experimental posttraumatic epilepsy.<sup>42</sup> Here, we showed that a generalized SE provokes time-dependent amyloidogenic and tau-related signatures in the hippocampus. Of all the markers examined, only BACE1 (Figure 2G) and AT100 (Figure 2B) were overexpressed long-term in this setting. GSK-3 $\beta$ (Tyr216) overexpression also persisted (Figure 3A). Although to a lesser extent than MTLE, a generalized SE is sufficient to trigger specific, time-dependent or transient, AD-relevant modifications. SE may represent a risk factor for a secondary sequel, similar to other acute head injuries.<sup>6,28,43–45</sup>

## 4.3 | Homeostatic control of inflammation intertwines with expression of AD-relevant markers during seizures

The reported AD-relevant trajectories reciprocated pro- and anti-inflammatory changes. Here, we focused on the glucocorticoid system, measuring GR phosphorylation and corticosterone blood levels. Thus, in addition to its crucial role in stress response, GR is directly implicated and controls potent endogenous anti-inflammatory processes.<sup>23,46</sup> Post-SE, a quick proinflammatory reaction was paralleled and temporally surpassed by the activation of the endogenous anti-inflammatory GR system. The latter was perhaps involved in curbing the SE-induced neurodegenerative trajectories.<sup>11,47</sup> Conversely, the GR system did not engage in the MTLE model, where

the proinflammatory changes persisted. These dissimilarities may result from the contrasting seizure progression patterns in the two models and are contingent on the extent of tissue lesions. As previously proposed for other neurological diseases,<sup>47</sup> epileptogenesis and recurrent seizures could induce a prolonged suprathreshold activation of the GR system, resulting in its desensitization over time. This pattern shares elements of similarity with the J20 mice (Figures 6 and 7A) and a model of amyloid toxicity induced by the intracerebroventricular injection of an oligomeric solution of A $\beta$ .<sup>21,23,48</sup> Within this framework, targeting the GR system could represent a strategy to reestablish the homeostatic control of inflammation, limiting neurodegenerative trajectories during seizures.<sup>49,50</sup>

## 4.4 | Open questions and limitations

Our study leaves several unsolved questions, and it offers a venue for further research. We acknowledge that GR activation may also indicate a prolonged stress response, which is logical in these experimental settings. Furthermore, MTLE and SE showed different or opposite effects on corticosterone levels and pGR/GR ratio (Figure 6), suggesting an association with seizure profiles in the two models.

Finally, in the generalized SE model, the ip KA injection can directly activate regions other than the hippocampus and involved in stress response, such as the hypothalamus, amygdala, and the medial frontal cortex.

Significantly, local tissue damage and considerable cellular injury are associated with the unilateral ih microinjection of KA, differently from the SE model or APP J20 mice. In general, the relevance of tissue damage (extent and evolution over time), particularly in the hippocampus, should be carefully studied, as it could significantly impact neurodegenerative and immune trajectories. However, we reported tau-related modifications in the nonlesional contralateral MTLE hippocampi, supporting the role of seizure activity. Furthermore, (1) single mouse tracking could unveil precise correlations between quantitative EEG patterns and brain pathophysiological modifications; (2) examining regions other than the hippocampus could further indicate the pathological value of seizure propagating regions and the role of the lesion; (3) the number of animals in each cage may have an impact (e.g., stress) on the reported outcomes, necessitating further investigations; and (4) targeting specific neurodegenerative and associated neuroinflammatory players could be disease-modifying or antiepileptogenic. Importantly, genetic reduction of endogenous tau levels protected against excitotoxicity induced by seizures.<sup>51–53</sup>

## 5 | CONCLUSIONS

In summary, our study shows that seizures promote tau hyperphosphorylation and amyloidogenic markers in the hippocampus, associated with inflammatory dysregulations over time. We have highlighted that a generalized SE could represent a risk factor for a neuropathophysiological trajectory. We showed the pathological value of lesional and nonlesional epileptogenic and seizure propagating brain regions.

### ACKNOWLEDGMENTS

This work was supported by ANR-Epicyte, ANR-EpiCatcher, and ANR/Era-Net Neu-Vasc (N.M.); by France Alzheimer, MUSE-GAiA University of Montpellier, and FRM-OPA (L.G.); and by LABEX-LipSTIC (C.D. and L.G.). G.C. and C.H. are supported by a Ph.D. grant from the University of Montpellier, France (CBS2 program). G.C. is also supported by a PhD Grant from the Center of Excellence in Neurodegenerative Disorders and C.H. by an exchange program from the Fondation Vaincre Alzheimer. We are very grateful to the late Dr Peter Davies (Feinstein Institute for Medical Research in Manhasset, NY, USA) for the generous gift of anti-tau antibodies.

### CONFLICT OF INTEREST

None of the authors has any conflict of interest to disclose. We confirm that we have read the Journal's position on issues involved in ethical publication and affirm that this report is consistent with those guidelines.

### ORCID

Geoffrey Canet  <https://orcid.org/0000-0001-7291-4512>  
 Laurent Givalois  <https://orcid.org/0000-0002-6698-5346>  
 Nicola Marchi  <https://orcid.org/0000-0001-9124-0226>

### REFERENCES

- Gourmaud S, Shou H, Irwin DJ, Sansalone K, Jacobs LM, Lucas TH, et al. Alzheimer-like amyloid and tau alterations associated with cognitive deficit in temporal lobe epilepsy. *Brain*. 2020;143:191–209.
- Tai XY, Koeppe M, Duncan JS, Fox N, Thompson P, Baxendale S, et al. Hyperphosphorylated tau in patients with refractory epilepsy correlates with cognitive decline: a study of temporal lobe resections. *Brain*. 2016;139:2441–55.
- Casillas-Espinosa PM, Ali I, O'Brien TJ. Neurodegenerative pathways as targets for acquired epilepsy therapy development. *Epilepsia Open*. 2020;5:138–54.
- Romoli M, Sen A, Parnetti L, Calabresi P, Costa C. Amyloid-beta: a potential link between epilepsy and cognitive decline. *Nat Rev Neurol*. 2021;17:469–85.
- Silva JC, Vivash L, Malpas CB, Hao Y, McLean C, Chen Z, et al. Low prevalence of amyloid and tau pathology in drug-resistant temporal lobe epilepsy. *Epilepsia*. 2021;62(12):3058–67.
- Joutsa J, Rinne JO, Hermann B, Karrasch M, Anttinen A, Shinnar S, et al. Association between childhood-onset epilepsy and amyloid burden 5 decades later. *JAMA Neurol*. 2017;74:583–90.
- Gan L, Cookson MR, Petrucelli L, La Spada AR. Converging pathways in neurodegeneration, from genetics to mechanisms. *Nat Neurosci*. 2018;21:1300–9.
- Boux F, Forbes F, Collomb N, Zub E, Mazière L, Bock F, et al. Neurovascular multiparametric MRI defines epileptogenic and seizure propagation regions in experimental mesiotemporal lobe epilepsy. *Epilepsia*. 2021;62(5):1244–55.
- Klement W, Blaquiere M, Zub E, deBock F, Boux F, Barbier E, et al. A pericyte-glia scarring develops at the leaky capillaries in the hippocampus during seizure activity. *Epilepsia*. 2019;60:1399–411.
- Klement W, Garbelli R, Zub E, Rossini L, Tassi L, Girard B, et al. Seizure progression and inflammatory mediators promote pericytosis and pericyte-microglia clustering at the cerebrovasculature. *Neurobiol Dis*. 2018;113:70–81.
- Zub E, Canet G, Garbelli R, Blaquiere M, Rossini L, Pastori C, et al. The GR-ANXA1 pathway is a pathological player and a candidate target in epilepsy. *FASEB J*. 2019;33:13998–4009.
- Runtz L, Girard B, Toussenet M, Espallergues J, Fayd'Herbe De Maudave A, Milman A, et al. Hepatic and hippocampal cytochrome P450 enzyme overexpression during spontaneous recurrent seizures. *Epilepsia*. 2018;59:123–34.
- Rusina E, Bernard C, Williamson A. The kainic acid model of temporal lobe epilepsy. *eNeuro*. 2021;8(2):ENEURO.0337-20.2021.
- Riban V, Boulleret V, Pham-Le BT, Fritschy JM, Marescaux C, Depaulis A. Evolution of hippocampal epileptic activity during the development of hippocampal sclerosis in a mouse model of temporal lobe epilepsy. *Neuroscience*. 2002;112:101–11.
- Mucke L, Masliah E, Yu GQ, Mallory M, Rockenstein EM, Tatsuno G, et al. High-level neuronal expression of abeta 1–42 in wild-type human amyloid protein precursor transgenic mice: synaptotoxicity without plaque formation. *J Neurosci*. 2000;20:4050–8.
- Canet G, Zussy C, Hernandez C, Chevallier N, Marchi N, Desrumaux C, et al. Chronic glucocorticoids consumption triggers and worsens experimental Alzheimer's disease-like pathology by detrimental immune-modulations. *Neuroendocrinology*. 2022. <https://doi.org/10.1159/000521559>
- Planel E, Richter KEG, Nolan CE, Finley JE, Liu L, Wen Y, et al. Anesthesia leads to tau hyperphosphorylation through inhibition of phosphatase activity by hypothermia. *J Neurosci*. 2007;27:3090–7.
- Mansuy M, Baille S, Canet G, Borie A, Cohen-Solal C, Vignes M, et al. Deletion of plasma phospholipid transfer protein (PLTP) increases microglial phagocytosis and reduces cerebral amyloid-beta deposition in the J20 mouse model of Alzheimer's disease. *Oncotarget*. 2018;9:19688–703.
- O'Leary TP, Savoie V, Brown RE. Learning, memory and search strategies of inbred mouse strains with different visual abilities in the Barnes maze. *Behav Brain Res*. 2011;216:531–42.
- Canet G, Chevallier N, Zussy C, Desrumaux C, Givalois L. Central role of glucocorticoid receptors in Alzheimer's disease and depression. *Front Neurosci*. 2018;12:739.



21. Pineau F, Canet G, Desrumaux C, Hunt H, Chevallier N, Ollivier M, et al. New selective glucocorticoid receptor modulators reverse amyloid-beta peptide-induced hippocampus toxicity. *Neurobiol Aging*. 2016;45:109–22.
22. Zussy C, Brureau A, Keller E, Marchal S, Blayo C, Delair B, et al. Alzheimer's disease related markers, cellular toxicity and behavioral deficits induced six weeks after oligomeric amyloid-beta peptide injection in rats. *PLoS One*. 2013;8:e53117.
23. Canet G, Pineau F, Zussy C, Hernandez C, Hunt H, Chevallier N, et al. Glucocorticoid receptors signaling impairment potentiates amyloid-beta oligomers-induced pathology in an acute model of Alzheimer's disease. *FASEB J*. 2020;34:1150–68.
24. Andorfer C, Kress Y, Espinoza M, De Silva R, Tucker KL, Barde Y-A, et al. Hyperphosphorylation and aggregation of tau in mice expressing normal human tau isoforms. *J Neurochem*. 2003;86:582–90.
25. Sculier C, Gainza-Lein M, Sanchez Fernandez I, Loddenkemper T. Long-term outcomes of status epilepticus: a critical assessment. *Epilepsia*. 2018;59(Suppl 2):155–69.
26. Neely CLC, Pedemonte KA, Boggs KN, Flinn JM. Nest building behavior as an early indicator of behavioral deficits in mice. *J Vis Exp*. 2019;152(e60139):1–8. <https://doi.org/10.3791/60139>
27. Arango-Lievano M, Boussadia B, De Terdonck LDT, Gault C, Fontanaud P, Lafont C, et al. Topographic reorganization of cerebrovascular mural cells under seizure conditions. *Cell Rep*. 2018;23:1045–59.
28. Tan SH, Karri V, Tay NWR, Chang KH, Ah HY, Ng PQ, et al. Emerging pathways to neurodegeneration: dissecting the critical molecular mechanisms in Alzheimer's disease, Parkinson's disease. *Biomed Pharmacother*. 2019;111:765–77.
29. Vaillant-Beuchot L, Mary A, Pardossi-Piquard R, Bourgeois A, Lauritzen I, Eysert F, et al. Accumulation of amyloid precursor protein C-terminal fragments triggers mitochondrial structure, function, and mitophagy defects in Alzheimer's disease models and human brains. *Acta Neuropathol*. 2021;141:39–65.
30. Vezzani A, Balosso S, Ravizza T. Neuroinflammatory pathways as treatment targets and biomarkers in epilepsy. *Nat Rev Neurol*. 2019;15:459–72.
31. Minjarez B, Camarena HO, Haramati J, Rodríguez-Yañez Y, Mena-Munguía S, Buriticá J, et al. Behavioral changes in models of chemoconvulsant-induced epilepsy: a review. *Neurosci Biobehav Rev*. 2017;83:373–80.
32. Rattka M, Brandt C, Loscher W. The intrahippocampal kainate model of temporal lobe epilepsy revisited: epileptogenesis, behavioral and cognitive alterations, pharmacological response, and hippocampal damage in epileptic rats. *Epilepsy Res*. 2013;103:135–52.
33. Monti G, Tondelli M, Giovannini G, Bedin R, Nichelli PF, Trenti T, et al. Cerebrospinal fluid tau proteins in status epilepticus. *Epilepsy Behav*. 2015;49:150–4.
34. Shahim P, Rejdak R, Ksiazek P, Blennow K, Zetterberg H, Mattsson N, et al. Cerebrospinal fluid biomarkers of beta-amyloid metabolism and neuronal damage in epileptic seizures. *Eur J Neurol*. 2014;21:486–91.
35. Sweeney MD, Kisler K, Montagne A, Toga AW, Zlokovic BV. The role of brain vasculature in neurodegenerative disorders. *Nat Neurosci*. 2018;21:1318–31.
36. Wu JW, Hussaini SA, Bastille IM, Rodriguez GA, Mrejeru A, Rilett K, et al. Neuronal activity enhances tau propagation and tau pathology in vivo. *Nat Neurosci*. 2016;19:1085–92.
37. Ascoli M, Ferlazzo E, Gasparini S, Mastroianni G, Citraro R, Roberti R, et al. Epidemiology and outcomes of status epilepticus. *Int J Gen Med*. 2021;14:2965–73.
38. Horvath L, Fekete I, Molnar M, Valoczy R, Marton S, Fekete K. The outcome of status epilepticus and long-term follow-up. *Front Neurol*. 2019;10:427.
39. Yan X-X, Cai Y, Zhang X-M, Luo X-G, Cai H, Rose GM, et al. BACE1 elevation is associated with aberrant limbic axonal sprouting in epileptic CD1 mice. *Exp Neurol*. 2012;235:228–37.
40. Liang Z, Liu F, Iqbal K, Grundke-Iqbal I, Gong CX. Dysregulation of tau phosphorylation in mouse brain during excitotoxic damage. *J Alzheimers Dis*. 2009;17:531–9.
41. Kodam A, Ourdev D, Maulik M, Hariharakrishnan J, Banerjee M, Wang Y, et al. A role for astrocyte-derived amyloid beta peptides in the degeneration of neurons in an animal model of temporal lobe epilepsy. *Brain Pathol*. 2019;29:28–44.
42. Liu S-J, Zheng P, Wright DK, Dezsai G, Braine E, Nguyen T, et al. Sodium selenate retards epileptogenesis in acquired epilepsy models reversing changes in protein phosphatase 2A and hyperphosphorylated tau. *Brain*. 2016;139:1919–38.
43. Ramos-Cejudo J, Wisniewski T, Marmar C, Zetterberg H, Blennow K, de Leon MJ, et al. Traumatic brain injury and Alzheimer's disease: the cerebrovascular link. *EBioMedicine*. 2018;28:21–30.
44. Ichkova A, Rodriguez-Grande B, Zub E, Saudi A, Fournier M-L, Aussudre J, et al. Early cerebrovascular and long-term neurological modifications ensue following juvenile mild traumatic brain injury in male mice. *Neurobiol Dis*. 2020;141:104952.
45. Sen A, Jette N, Husain M, Sander JW. Epilepsy in older people. *Lancet*. 2020;395:735–48.
46. Meijer OC, Koorneef LL, Kroon J. Glucocorticoid receptor modulators. *Ann Endocrinol*. 2018;79:107–11.
47. Vandewalle J, Luypaert A, De Bosscher K, Libert C. Therapeutic mechanisms of glucocorticoids. *Trends Endocrinol Metab*. 2018;29:42–54.
48. Brureau A, Zussy C, Delair B, Ogier C, Ixart G, Maurice T, et al. Deregulation of hypothalamic-pituitary-adrenal axis functions in an Alzheimer's disease rat model. *Neurobiol Aging*. 2013;34:1426–39.
49. Van Bogaert T, Vandevyver S, Dejager L, Van Hauwermeiren F, Pinheiro I, Petta I, et al. Tumor necrosis factor inhibits glucocorticoid receptor function in mice: a strong signal toward lethal shock. *J Biol Chem*. 2011;286:26555–67.
50. Coutinho AE, Chapman KE. The anti-inflammatory and immunosuppressive effects of glucocorticoids, recent developments and mechanistic insights. *Mol Cell Endocrinol*. 2011;335:2–13.
51. Roberson ED, Scarce-Levie K, Palop JJ, Yan F, Cheng IH, Wu T, et al. Reducing endogenous tau ameliorates amyloid beta-induced deficits in an Alzheimer's disease mouse model. *Science*. 2007;316:750–4.
52. Jones NC, Nguyen T, Corcoran NM, Velakoulis D, Chen T, Grundy R, et al. Targeting hyperphosphorylated tau with

sodium selenate suppresses seizures in rodent models. *Neurobiol Dis.* 2012;45:897–901.

53. DeVos SL, Goncharoff DK, Chen G, Kebodeaux CS, Yamada K, Stewart FR, et al. Antisense reduction of tau in adult mice protects against seizures. *J Neurosci.* 2013;33:12887–97.

### SUPPORTING INFORMATION

Additional supporting information may be found in the online version of the article at the publisher's website.

**How to cite this article:** Canet G, Zub E, Zussy C, Hernandez C, Blaquiere M, Garcia V, et al. Seizure activity triggers tau hyperphosphorylation and amyloidogenic pathways. *Epilepsia.* 2022;63:919–935. <https://doi.org/10.1111/epi.17186>